IEEE Access
Multidisciplinary | Rapid Review | Open Access Journal

Received November 27, 2020, accepted December 6, 2020, date of publication December 9, 2020,
date of current version December 29, 2020.

Digital Object Identifier 10.1109/ACCESS.2020.3043542

A Paced-ECG Detector and Delineator for Automatic Multi-Parametric Catheter Mapping of Ventricular Tachycardia

PHILIP HOYLAND[1,2], NÉFISSA HAMMACHE[3], ALBERTO BATTAGLIA[3], JULIEN OSTER[1], JACQUES FELBLINGER[1,4], (Member, IEEE), CHRISTIAN DE CHILLOU[1,3], AND FREDDY ODILLE[1,4]

[1]IADI U1254, Inserm and Université de Lorraine, 54000 Nancy, France
[2]Biosense Webster France, Johnson & Johnson, 92130 Issy-les-Moulineaux, France
[3]Pôle Cardiologie, CHRU Nancy, 54000 Nancy, France
[4]CIC-IT 1433, Inserm, Université de Lorraine and CHRU Nancy, 54000 Nancy, France

Corresponding author: Philip Hoyland (phoyland@its.jnj.com)

This work was supported by the French "Investments for the Future" Program under Grant ANR-15-RHU-0004.

ABSTRACT Ventricular tachycardia (VT) is a life-threatening arrhythmia, which can be treated by catheter intervention. Accurate identification of the underlying reentrant circuit is often challenging, yet it is key to successful ablation of the VT. In practice, the cardiologist often uses electrocardiography (ECG) data provided by various catheter mapping techniques, including parameters acquired during sinus rhythm (voltage maps, presence of fragmented/late potentials) and during controlled pacing from different sites of the ventricle, so-called pace-mapping. A novel method is presented here to automatically extract the key information from pace-mapping data with automated detection of paced heartbeats from the surface ECG signals, using wavelet detection of pacing spikes and combined time/energy criteria, and automated delineation of paced beats, QRS peak, and QRS onset. This allows the generation of correlation gradient maps (indicating QRS morphology changes as the catheter is moved) and stimulus-to-QRS maps (sQRS, indicating the delay between pacing and activation of the healthy myocardium). The delineator is shown to be in good agreement with manual annotations from experts in a retrospective study of 18 VT ablation procedures. Paced-QRS detection had 95.2% sensitivity and 98.4% positive predictive value. Resulting sQRS maps had a mean absolute error of 11.1 ms, which was in the same range as the inter-observer errors (9.7 ms). The automatic processing drastically reduces the need for manual annotations. Therefore it makes it feasible to process and visualize, during the procedure, all the relevant parametric maps, which can be analyzed jointly to identify VT circuits and corresponding ablation targets.

INDEX TERMS Arrhythmia, cardiac interventional electrophysiology, electrocardiography, radiofrequency catheter ablation.

I. INTRODUCTION

After myocardial infarction, the presence of damaged tissue can modify the electrical propagation within the myocardium. Some areas do not conduct anymore and are responsible for directional block, whereas intermediate areas with sparse surviving myocardial fibers are responsible for slow conducting zones. The coupling of these two elements form the basis for reentrant ventricular tachycardia (VT) [1]. A reentrant VT circuit may indeed exist if there is a slow conducting zone from which the electrical influx exits with a delay greater than the myocyte refractory period, thus exciting healthy tissue again. VT is a life-threatening arrhythmia, which can be treated by catheter intervention provided the core zone of the underlying reentrant circuit can be identified accurately and ablated.

The most direct technique to identify the circuit is activation mapping [2]. It consists of creating a 3D map of the activation pathway during VT by moving the electrodes of a catheter and measuring the activation times from the

The associate editor coordinating the review of this manuscript and approving it for publication was Filbert Juwono.

intra-cardiac signals. Automatic activation mapping has been aided by the development of algorithmic delineation tools to automatically assess the local activation time of intracardiac atrial [3] as well as ventricular signals [4]. Unfortunately, in practice, activation mapping can only be performed in the small proportion of patients who can tolerate VT long enough for the duration of the mapping.

Noninvasive methods have also been developed to reconstruct the electrical activation sequences of the ventricle. These techniques are based on analyzing the ECG morphology during tachycardia to help the physician determine the area of interest [5]. This information can therefore help reduce the searching area, thus leading to shorter procedure times. However, some technical challenges remain especially as some features seem to be inaccurately captured [6]. Further clinical benefit remains to be shown for the widespread adoption of this technique [7].

Alternative indirect methods consist of collecting data during sinus rhythm and during catheter-controlled pacing from different sites of the ventricle (so-called pace-mapping) to study the local electrical characteristics of the ventricle and attempt to identify the critical components of the VT circuit.

Sinus rhythm measurements include voltage mapping, which maps the amplitude of the intracardiac electrical signals (electrograms). High voltage measurements correspond to viable myocardial fibers and low voltage to tissues with impaired electrical conductivity. Intermediate voltage characterized by abnormal electrograms correspond to surviving myocardial fibers [8][9]. The recent development of high-density mapping catheters enables the detection of late or fragmented potentials. The elimination of such electrograms has been assessed as a procedural endpoint [10]. Unfortunately, a disadvantage of such a technique is that it induces larger tissue destruction than would be required if the actual VT circuits could be accurately identified.

Pace-mapping data include surface electrocardiography (ECG) signals collected during pacing from many sites of the ventricle. They can be used to determine the VT circuit. Indeed, the exit site of the VT circuit is identified when the paced QRS morphology best matches that of the clinical VT [11], as assessed by a VT correlation map. A drawback of VT correlation mapping is that it requires a reference ECG recording during VT (spontaneous or induced at the beginning of the procedure). However secondary VT circuits may also exist and are not mapped by this technique. Reference-less pace mapping has also been proposed to identify critical slow conducting zones, independently of any VT recording (i.e. potentially core zones of several VT circuits) [12]. It uses correlation gradient maps, indicating zones of abrupt changes on the surface ECG as the catheter is moved to neighboring ventricular sites. Additionally, the entrance of the circuit has been shown to be associated with long (or longer) intervals between pacing and the resulting QRS complex (sQRS intervals) [13]. A combined analysis of these multi-parametric pace-mapping data may therefore help better identify all likely VT circuits for one patient and determine the minimal surface where tissue destruction needs to be applied.

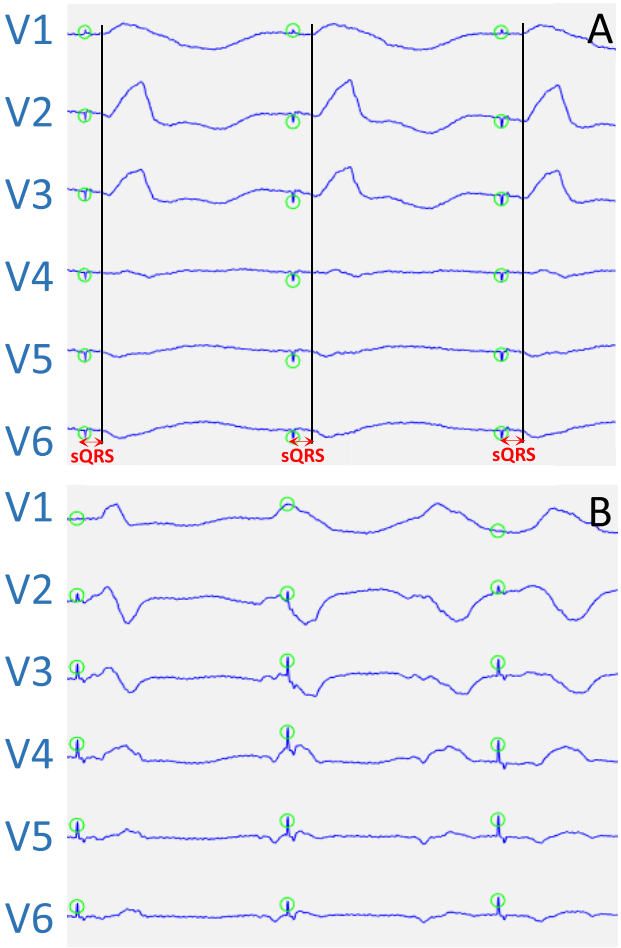

FIGURE 1. Illustration of the 6 precordial leads of two different pacing sites. The green circle represents the pacing spike. In A, the black line represents the beginning of the QRS and the red arrow is the sQRS interval, the time interval between both features. The three QRS present the same morphology as well as the same sQRS interval, therefore they can be identified as three correctly paced QRS. In B, this is not the case, the beats cannot be considered as paced and mustn't be analyzed.

Currently, the use of pace-mapping data is coupled with time-consuming manual steps. Firstly, it is important to quickly identify a correctly paced QRS. For example, bad catheter to tissue contact and poor local electrical activity can lead to defaults in tissue capture. The subsequent non-paced QRS complexes must not be analyzed. As illustrated in Fig. 1, a paced beat can be easily identified by a constant delay between the stimulation spike and the QRS onset, i.e. a constant sQRS interval, as well as a constant QRS morphology (same overall electrical depolarization induced by the stimulation). The spike as well as the start of the QRS need to be detected in order to determine the valuable sQRS intervals. The lack of already implemented detection techniques hinder the current use of pace-mapping data in clinical practice.

Pacing spike detection in patients with pacemakers has already been developed using slope based [14]–[16] and power envelopes with moving statistical windows [17] detection algorithms but to our knowledge these methods have not been used for catheter pacing. Convolution with a spike template has already been used in [12] for catheter induced pacing detection but the application of this method is complicated by the varying amplitude of the stimulus as well as the great diversity in localization of the pacing. The spike frequency range being higher than the frequency of the other features present on the ECG, we propose a new wavelet-based method for detecting pacing spikes in a catheter-induced pacing environment. Moreover, conventional ECG signal processing techniques are developed for natural recordings (sinus rhythm or spontaneous arrhythmia) and have not been applied to detect and delineate catheter-paced beats [18]–[20].

Therefore in this work we propose a specific and innovative method for catheter paced-ECG data, combining a wavelet-based detection of stimulation spikes and a delineation of the subsequent QRS complex (peak and onset).

The objective of the study is to evaluate the performance of the proposed paced-ECG detection and delineation and to demonstrate its potential for multi-parametric catheter mapping of VT in the clinical setting. The overall goal is to provide the interventional cardiologist with a software tool to rapidly visualize the relevant maps (voltage, correlation and sQRS) and identify the potential VT circuit(s) to be ablated.

II. METHODS

A. PATIENT DATA ACQUISITION

Thirteen patients (9 men, mean age = 59 ± 12 years) consecutively referred for post-infarct VT catheter ablation between March 2016 and October 2017 were included in this retrospective, non-interventional study. Inclusion criteria were: (i) spontaneous sustained monomorphic VT inducible during the electrophysiological study; (ii) identification of the VT isthmus by the pace-mapping technique and (iii) radiofrequency catheter ablation lesions along the isthmus prevented VT induction. The study complied with the declaration of Helsinki and all procedures complied with the CHRU-Nancy guidelines. All 18 procedures were performed with the CARTO3®(Biosense Webster, Inc., Irvine, USA) and the Niobe®system (Stereotaxis Inc., St. Louis, USA).

Anonymized data were exported from the CARTO3® workstation and were then processed using an in-house software written in MATLAB language (The Mathworks, Natick, USA), version R2020a. Electro-anatomic data were first loaded into the software, including: catheter positions and 2.5 s of 12-lead ECG data acquired for each pace-mapping site; high-resolution vendor-generated 3D meshes of the ventricular cavity, as well as bipolar and unipolar voltage maps acquired in sinus rhythm. All other maps used in this study were generated offline with the MATLAB software, as described henceforth.

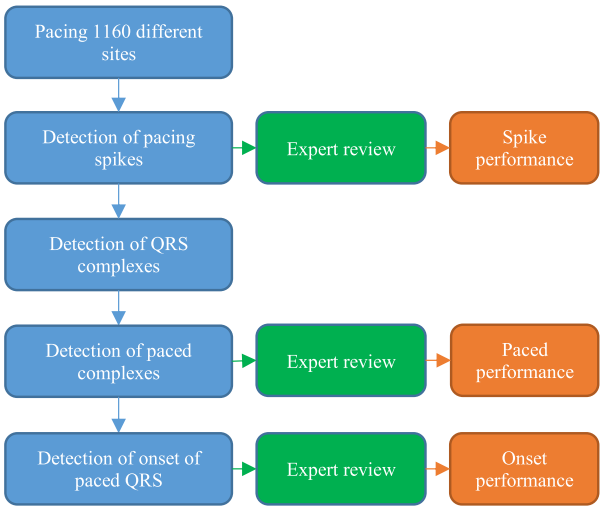

FIGURE 2. Flow diagram presenting the different steps of the detection algorithm.

B. AUTOMATED DETECTION AND DELINEATION OF PACE-ECG DATA

To analyze pace-mapping ECG data, an automatic detection and delineation of paced beats was proposed in order to only select one paced QRS for analysis at a given pacing site. This detection is necessary because some QRS complexes at a given site are not paced. The cardiac electric potentials can be expressed in vector quantities that varies over time in magnitude and direction. The overall projection of the human equivalent heart dipole in three orthogonal axes is the vectorcardiogram [21]. The maximum of its module correspond to the peak of depolarization of cardiac cells, thus useful to detect the QRS complex.

Moreover, the stimulation spike does not always induce a paced beat, especially in low-voltage hard to capture areas. Finally, mechanically induced premature beats must not be taken into account.

Figure 2 presents the different steps of the automated detection and delineation (i.e. determination of QRS peak and onset):

1. Detection of pacing spikes by using the continuous wavelet transform (CWT). The bump wavelet was selected as the mother wavelet for its frequency localization properties. The CWT was computed numerically using Matlab's *cwt* function, which uses L1 normalization of the coefficients, instead of L2 normalization in the integral definition of the CWT. This makes the time-frequency analysis easier as oscillatory components with the same amplitude in the signal always have the same magnitude in the CWT (independent of the scale). The wavelet coefficients $c_i(.)$ for each lead i corresponding to frequencies between $f_1 = 125$ Hz and $f_2 = 166$ Hz were summed in a signal S:

$$S = \sum_{i=1}^{12} \sum_{f \in \{f_1, \ldots, f_2\}} |c_i(f)| \quad (1)$$

The local maxima of S were extracted using Matlab's *findpeaks* function, with the following constrains: local maxima should reach at least 33% of the maximum of S, and two peaks should be separated by at least 350 ms. Overall 5138 spikes were analyzed.

2. Detection of QRS complexes present after each spike n using a maximum search of the vectorcardiogram. The synthetic vectorcardiogram $VCG(t)$, for a given time t, was reconstructed by inverse Dower transformation T from the available (independent) leads $L(t)$ [22] as already used in [12] (2), as shown at the bottom of the page. The time $t_{QRS,n}$ of the QRS complex after spike n was determined by the maximum of the module of the vectorcardiogram $\|VCG(t)\|$ between time t_n of spike n and time t_{n+1} of spike $n+1$:

$$t_{QRS,n} = \underset{\substack{t \\ for\ t\in[t_n,t_{n+1}[}}{\arg\max} \|VCG(t)\| \tag{3}$$

3. Determination of a paced-QRS flag by analysis of the previous QRS. A QRS was considered to be a paced QRS if similar to the previous one; similarity was defined by a distance-to-spike variation lower than 35 ms and a variation in the module of the vectorcardiogram below 33%. Overall 5176 QRS were present, of whom 2991 were paced.
4. Detection of the onset of a QRS by using the module of the vectorcardiogram. The QRS start was determined by backward search from the maximum of the VCG amplitude, until the module reached 5% of the maximum module.

The time interval between pacing and the start of the resulting QRS complex, the sQRS interval, was finally determined. The dataset was split between a training set consisting of the first 5 patients and a test set with the data from the remaining 13 patients. The optimization process was performed on the training set by tuning the 4 parameters (33% for pacing spike detection, the similarity criteria of 35 ms and 33% for paced beat detection and 5% for onset delineation) using a grid search. The parameters were chosen only based on the training set and then evaluated once on the test set.

Overall, bipolar pace-mapping was performed at 1160 different sites. It should be noted that several QRS complexes are present in each 2.5 s recording (i.e. at one given pacing site). For each site, the second QRS in the sequence of QRS identified as paced by the algorithm was studied.

C. VALIDATION AGAINST EXPERT ANOTATIONS

The software tool allowed visualization of all the automatically detected QRS signals. An experienced interventional cardiologist (N.H.) was asked to review the ECG signals (pacing spike, whether a QRS was paced or not). The efficiency of the automated processing was assessed by common statistics for binary classifiers (using the cardiologist input as the ground truth), including the positive predictive value (PPV) and the sensitivity (Se). The position of the QRS onset varies slightly between cardiologists. To quantify this inter-observer variation, two experts were asked to mark the QRS onset: a clinical support specialist (P.H) defined as expert 1 and an interventional cardiologist (N.H.) defined as expert 2. We also introduced a virtual delineation represented by the mean of both experts. Mean, standard deviation, median and mean absolute errors were calculated for the definition of the QRS onset time. The agreement between expert and automated S-QRS maps was also assessed by correlation analysis (using both Spearman's and Lin's definitions) and by Bland-Altman analysis.

D. RECONSTRUCTION OF MULTI-PARAMETRIC MAPS

Multiple 3D maps were generated to visualize the information. The bipolar voltage map was directly derived from the vendor's CARTO3®software. Additionally, a 3D surface mesh was generated from the pacemapping sites and used to create the following maps: (i) a sQRS interval map was generated by color-coding the sQRS interval induced by the pacing stimuli; (ii) a reference-less correlation gradient map was generated as described in [12] by calculating the local change in Pearson correlation coefficient $c(.,.)$ between each lead of QRS complexes from two neighboring pacing sites, x_1 and x_2, $S^{lead}_{PacedQRS}(x_1)$ and $S^{lead}_{PacedQRS}(x_2)$ normalized by the distance between the two sites $||x_1 - x_2||$:

$$\frac{\frac{1}{12}\sum_{lead=1}^{12} c\left(S^{lead}_{PacedQRS}(x_1) - S^{lead}_{PacedQRS}(x_2)\right)}{||x_1 - x_2||} \tag{4}$$

The target for the clinician was to collect points with a distance of 10 mm in areas of low voltage. The distance between two points was higher in healthy areas. Correlation gradient values were considered to be defined only when the site-to-site distance was less than 20 mm. The rationale for computing these three maps is that sQRS maps are expected to highlight VT circuit entrance sites [13] and correlation gradient maps are expected to highlight VT circuit core zones [12]. Finally, voltage maps are expected to help identify

$$\begin{aligned} VCG(t) &= T * L(t)^T, \\ L(t) &= [V_1(t)\, V_2(t)\, V_3(t)\, V_4(t)\, V_5(t)\, V_6(t)\, I(t)\, II(t)], \\ T &= \begin{bmatrix} -0.172 & -0.074 & 0.122 & 0.231 & 0.236 & 0.194 & 0.156 & -0.010 \\ 0.057 & -0.019 & -0.106 & -0.022 & 0.041 & 0.048 & -0.227 & 0.887 \\ -0.229 & -0.310 & -0.246 & -0.063 & 0.055 & 0.108 & 0.022 & 0.102 \end{bmatrix} \end{aligned} \tag{2}$$

TABLE 1. Performance of the Proposed Detection of Stimulation Spikes and Paced QRS Complexes.

	Training set		Test set		Training and Test set	
	Sensitivity	Positive Predictive value	Sensitivity	Positive Predictive value	Sensitivity	Positive Predictive value
Spike detector	97.64%	98.86%	97.48%	99.61%	97.51%	99.46%
Paced QRS detector	94.99%	97.69%	95.23%	98.63%	95.19%	98.44%

TABLE 2. Onset Performance Results.

	Training set				Test set				Training and Test set			
	Mean	Standard Deviation	Median	Mean Absolute Error	Mean	Standard Deviation	Median	Mean Absolute Error	Mean	Standard Deviation	Median	Mean Absolute Error
Between algorithm and expert 1	-2.36ms	21.99ms	-4ms	15.71ms	-1.19ms	16.14ms	-2ms	10.89ms	-1.42ms	17.43ms	-3ms	11.82ms
Between algorithm and expert 2	4.65ms	21.37ms	3ms	14.34ms	0.13ms	17.12ms	-2ms	11.30ms	1.01ms	18.11ms	-1ms	11.88ms
Between algorithm and mean delineation of both experts	1.15ms	20.65ms	-0.5ms	13.71ms	-0.53ms	15.37ms	-2ms	10.30ms	-0.21ms	16.54ms	-2ms	10.96ms
Between the two experts	7.01ms	13.21ms	7ms	11.77ms	1.32ms	12.74ms	1ms	9.25ms	2.42ms	13.03ms	+2ms	9.73ms

the exit of the VT circuit, which should be at the border between scar and healthy tissue.

For better visualization purpose, the maps were finally projected from the coarse mesh formed by pacing sites onto the high-resolution anatomical mesh (distance between the vertices was 0.8mm) provided by the vendor (using nearest-neighbor interpolation). For final visualization of the 3D maps, the rendering engine (still within MATLAB in this study) was set to use interpolation of values defined at each vertex of the high resolution mesh, similarly to the vendor's CARTO3®software.

III. RESULTS

A. PACED-QRS DETECTION AND DELINEATION

Quantitative results for the automatic detection of pacing spikes and paced QRS complexes are summarized in Table 1. The performance was very similar between the training set, the test set and the entire study population (training and test). The overall results for the entire population show excellent agreement between the algorithm and the cardiologist, with Se>95% and PPV>98%.

Regarding the detection of the QRS onset, quantitative results on the training, test and entire population set are summarized in Table 2. The onset algorithm performed better on the test set than on the training set. For 94% of QRS onset detections, a difference lower than 30 ms was found between expert 2 and the algorithm inputs. The difficulty of defining an objective location for the beginning of the QRS complex is highlighted by the relatively large mean absolute error between the two experts (9.73 ms). When compared to the delineation represented by the mean of both experts, the proposed algorithm performed well (mean of −0.21 ms, a SD of 16.54 ms, a MED of −2 ms and a MAE of 10.96 ms) and demonstrated only a slightly higher difference than between both experts.

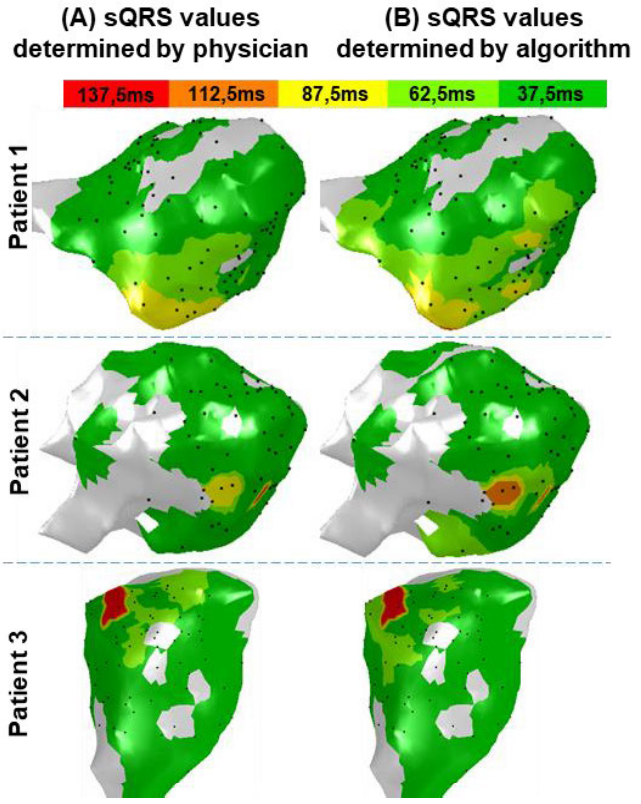

FIGURE 3. Comparison of left ventricle SQRS maps determined between (A) the physician (N.H) and (B) the algorithm. For each patient, both maps indicate the same interesting zones with longer SQRS intervals.

B. RECONSTRUCTION OF MULTIPARAMETRIC MAPS

The delay between the stimulation spike and the QRS onset, the sQRS interval, was calculated for each pacing site and projected onto the high-resolution anatomical mesh. Figure 3 shows examples of sQRS interval maps generated by values determined by the physician N.H. in comparison with values determined by the proposed algorithm.

TABLE 3. Final Visualization Vertex Results Between s-QRS Maps Generated by Algorithm and Physician Inputs of the Test Set.

	Mean	Standard deviation	Median	Mean Absolute Error	Spearman's correlation	Lin's correlation
Between algorithm and expert 1	-1.95ms	14.80ms	-2ms	10.06ms	0.71	0.86
Between algorithm and expert 2	0.15ms	15.46ms	-1ms	10.64ms	0.72	0.86
Between the two experts	2.10ms	13.92ms	1ms	9.26ms	0.75	0.88

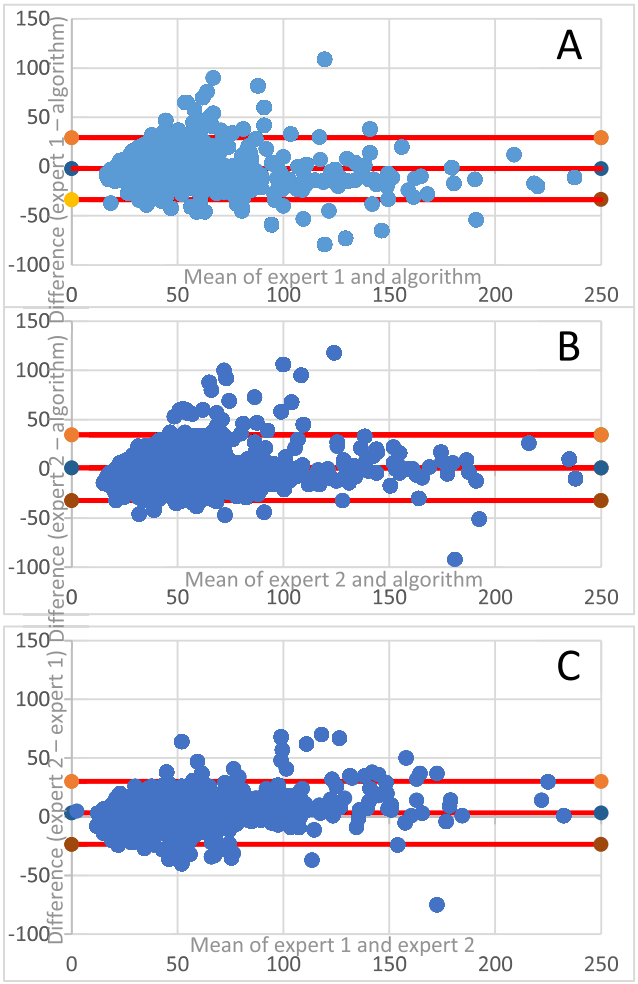

FIGURE 4. Bland Altman plot of agreement between methods. The lower red line represent the average difference −1,96 times the standard deviation of the difference, the middle red line the average difference and the upper red line the average difference +1,96 times the standard deviation of the difference. (A) between inputs from expert 1 and algorithm (B) between inputs from expert 2 and algorithm (C) between inputs from expert 2 and expert 1.

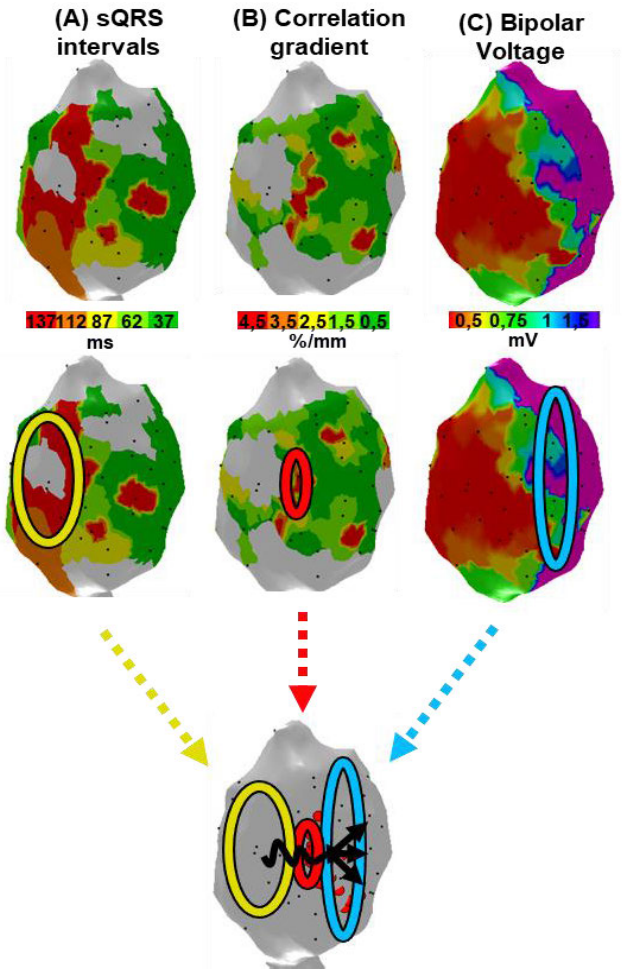

FIGURE 5. Illustration of the possible identification steps using maps calculated by the algorithm to determine the location of the critical section of the VT circuit or isthmus: (A) sQRS intervals, with longest values in red; the yellow circle includes the highest sQRS values and is likely located at the entrance of the isthmus (B) correlation gradient map indicating in red zones a high morphology mismatch; the red circle includes the highest values, likely located in the mid-isthmus section (C) bipolar voltage map, with low voltage in red representing the scar region and purple representing the healthy area; the blue circle includes the border between scar and healthy tissue, likely located at the exit of the isthmus.

The resulting QRS maps using the physician and the algorithm inputs looked very similar. Both versions of the maps enabled the quick identification of areas of interest marked by long sQRS intervals.

Quantitative differences between the detector-generated sQRS maps and the physician-generated sQRS maps, as assessed by vertex-wise differences and by correlation analysis between the final visualization meshes from the test set are summarized in Table 3. Bland-Altman plots (figure 4) show a good agreement between experts and the algorithm. The linear interpolation, which was used to reconstruct the final high resolution meshes, further decreased the impact of the difference between the algorithm and the experts' annotations.

Figure 5 shows an example of multi-parametric mapping (3 maps) of the same patient. The sQRS interval map (A)

and the correlation gradient map (B) were generated using the algorithm generated values. The bipolar voltage map (C) was derived from the CARTO3®software. The visualization of this multi-parametric mapping may help to determine the localization of the entrance, core and exit of the VT circuit.

IV. DISCUSSION

The objective of a VT ablation procedure is to identify the main components of all the fast reentrant circuits the patient is capable of sustaining. Activation mapping during tachycardia is the most direct technique but can only be performed in the small proportion of patients who can tolerate VT long enough for the duration of the mapping. Furthermore it only identifies the principal VT circuit, i.e. it does not identify secondary VT circuits that may occur after ablation of the principal one. The analysis of data collected during sinus rhythm and pace-mapping enables the detailed study of the local electrical characteristics of the ventricle. Currently, this type of analysis is limited because of the high number and time-consuming steps that the physician needs to do. Once the physician is stable in a position and starts pacing, a point is taken. The necessary manual steps are the following: selecting a correctly paced beat, determining the position of the pacing spike and onset of the QRS, calculating the difference to establish the sQRS interval, aligning the QRS morphology of the point regarding the QRS morphology of its closest neighbors. In order to integrate this full workflow and take full advantage of pace map data, we have estimated that the physician currently needs 30 seconds per point, adding up to 50 minutes for 100 pace map points. The added value of an automated algorithm is to facilitate the use of the data. Out of 100 pace map points, the proposed method correctly identifies 99 paced QRS. If we consider a tolerance threshold of 30 ms for the start of the QRS, only 6% of points will be incorrectly marked. All in all, for a 100 pace map points, 7 points will need to be corrected and 93 would be rapidly visualized for validation leading to a total time of less than 5 minutes. This time is short compared to the total procedure time of several hours and will help by making the time allocated to analyzing the data more predictable, leading to an increased standardization of the physician's approach to ischemic VT. Reviewing data is standard in clinical practice as it helps the physician determine the most effective ablation strategy. It is also important that the physician reviews all points because, in certain cases, although the algorithm performed well, the result will need to be modified. For example, after reviewing the surrounding paced beat morphologies, the physician might consider a beat as being correctly paced even if the recording does not have two consecutive beats with the same morphology.

The pace-mapping based method described here has the main advantage of being feasible in all patients, regardless of being able to induce a VT episode. Once the likely circuits are identified, ablation targets can be determined in order to eliminate the critical slow-conducting zones. Once ablated, these areas will not conduct anymore, thus preventing the reentrant circuit from forming and curing the patient.

The proposed software tool automatically creates voltage, correlation and sQRS maps. The creation of these multiparametric maps help determine the different characteristics of the VT isthmus. Previous articles have shown the importance of these parameters in identifying the isthmus. The isthmus is a complex structure and the visualization of a single parameter is not enough to be able to reconstruct the VT circuit. For each map, the global patterns with the highest and the lowest group of values are useful. Indeed it is important to know whether a sQRS is long (over 100 ms) or short (under 50 ms), thus the mean absolute error of 11.1 ms is low enough for the automatic sQRS maps to be analyzed. It is important to have a global approach and take into account all the relevant information before establishing a diagnosis. In this study only a qualitative analysis of the maps is presented, which is meant to show the added value of visualizing the maps together, rather than to provide a full clinical validation of the method.

The combination of the multi-parametric maps can bring to light multiple slow-conducting zones in the ventricle. These zones can then result in the creation of multiple tachycardia circuits. Highlighting the multiple isthmuses is of interest when elaborating a VT ablation strategy.

An increased understanding of VT circuits will lead to increased VT ablation results. The proposed study enables to automatically extract the relevant data. This data is acquired during sinus rhythm or pacing from the catheter and thus has the advantage of not requiring any tachycardia during acquisition. The data can therefore be easily obtained, not requiring any stimulating maneuvers with unpredictable results. If the VT can be induced and is well tolerated, activation data can also be automatically extracted and could further increase our understanding of the VT circuits.

Large datasets can now more easily be used as inputs for the development of future algorithms. These algorithms need to automatically determine all likely VT circuits, further facilitating the diagnosis and improving long-term ablation outcomes.

V. CONCLUSION

We developed a paced-ECG detector and delineator that is useful for multi-parametric catheter mapping. This automated method facilitates the creation and visualization of the relevant maps, which can be analyzed jointly to identify VT circuits and the corresponding ablation targets.

ACKNOWLEDGMENT

The authors would like to thank INSERM, CPER 2007–2013, Region Lorraine, and FEDER for the funding of the Niobe Magnetic Navigation System, Stereotaxis, Inc.

REFERENCES

[1] N. El-Sherif, B. J. Scherlag, R. Lazzara, and R. R. Hope, "Re-entrant ventricular arrhythmias in the late myocardial infarction period. 1. conduction characteristics in the infarction zone.," *Circulation*, vol. 55, no. 5, pp. 686–702, May 1977.

[2] W. G. Stevenson, H. Khan, P. Sager, L. A. Saxon, H. R. Middlekauff, P. D. Natterson, and I. Wiener, "Identification of reentry circuit sites during catheter mapping and radiofrequency ablation of ventricular tachycardia late after myocardial infarction," *Circulation*, vol. 88, no. 4, pp. 1647–1670, Oct. 1993.

[3] M. El Haddad, R. Houben, R. Stroobandt, F. Van Heuverswyn, R. Tavernier, and M. Duytschaever, "Algorithmic detection of the beginning and end of bipolar electrograms: Implications for novel methods to assess local activation time during atrial tachycardia," *Biomed. Signal Process. Control*, vol. 8, no. 6, pp. 981–991, Nov. 2013.

[4] A. Alcaine, D. Soto-Iglesias, M. Calvo, E. Guiu, D. Andreu, J. Fernandez-Armenta, A. Berruezo, P. Laguna, O. Camara, and J. P. Martinez, "A wavelet-based electrogram onset delineator for automatic ventricular activation mapping," *IEEE Trans. Biomed. Eng.*, vol. 61, no. 12, pp. 2830–2839, Dec. 2014.

[5] T. Yang, S. M. Pogwizd, G. P. Walcott, L. Yu, and B. He, "Noninvasive activation imaging of ventricular arrhythmias by spatial gradient sparse in frequency domain—Application to mapping reentrant ventricular tachycardia," *IEEE Trans. Med. Imag.*, vol. 38, no. 2, pp. 525–539, Feb. 2019.

[6] L. R. Bear, O. Bouhamama, M. Cluitmans, J. Duchateau, R. D. Walton, E. Abell, C. Belterman, M. Haissaguerre, O. Bernus, R. Coronel, and R. Dubois, "Advantages and pitfalls of noninvasive electrocardiographic imaging," *J. Electrocardiol.*, vol. 57, pp. S15–S20, Nov. 2019.

[7] M. Cluitmans, D. H. Brooks, R. MacLeod, O. Dössel, M. S. Guillem, P. M. van Dam, J. Svehlikova, B. He, J. Sapp, L. Wang, and L. Bear, "Validation and opportunities of electrocardiographic imaging: From technical achievements to clinical applications," *Frontiers Physiol.*, vol. 9, p. 1305, Sep. 2018.

[8] J. M. de Bakker, F. J. van Capelle, M. J. Janse, A. A. Wilde, R. Coronel, A. E. Becker, K. P. Dingemans, N. M. van Hemel, and R. N. Hauer, "Reentry as a cause of ventricular tachycardia in patients with chronic ischemic heart disease: Electrophysiologic and anatomic correlation.," *Circulation*, vol. 77, no. 3, pp. 589–606, Mar. 1988.

[9] A. Arenal, "Tachycardia-related channel in the scar tissue in patients with sustained monomorphic ventricular tachycardias: Influence of the voltage scar definition," *Circulation*, vol. 110, no. 17, pp. 2568–2574, 2004.

[10] P. Jais, P. Maury, and P. Khairy, "Elimination of local abnormal ventricular activities clinical perspective: A new end point for substrate modification in patients with scar-related ventricular tachycardia," *Circulation*, vol. 125, no. 18, pp. 2184–2196, 2012.

[11] C. de Chillou, L. Groben, I. Magnin-Poull, M. Andronache, M. M. Abbas, N. Zhang, A. Abdelaal, S. Ammar, J.-M. Sellal, J. Schwartz, B. Brembilla-Perrot, E. Aliot, and F. E. Marchlinski, "Localizing the critical isthmus of postinfarct ventricular tachycardia: The value of pace-mapping during sinus rhythm," *Heart Rhythm*, vol. 11, no. 2, pp. 175–181, Feb. 2014.

[12] F. Odille, A. Battaglia, P. Hoyland, J.-M. Sellal, D. Voilliot, C. de Chillou, and J. Felblinger, "Catheter treatment of ventricular tachycardia: A reference-less pace-mapping method to identify ablation targets," *IEEE Trans. Biomed. Eng.*, vol. 66, no. 11, pp. 3278–3287, Nov. 2019.

[13] A. Battaglia, F. Odille, I. Magnin-Poull, J.-M. Sellal, P. Hoyland, D. Hooks, D. Voilliot, J. Felblinger, and C. de Chillou, "An efficient algorithm based on electrograms characteristics to identify ventricular tachycardia isthmus entrance in post-infarct patients," *EP Europace*, vol. 22, no. 1, pp. 109–116, Nov. 2019.

[14] E. D. Helfenbein, J. M. Lindauer, S. H. Zhou, R. E. Gregg, and E. C. Herleikson, "A software-based pacemaker pulse detection and paced rhythm classification algorithm," *J. Electrocardiol.*, vol. 35, p. 95, Mar. 2002.

[15] I. I. Jekova, I. T. Iliev, V. V. Tsibulko, and S. D. Tabakov, "Algorithm for pace pulses detection in a single lead ECG: Performance in case of EMG artifacts," in *Proc. IEEE XXVII Int. Sci. Conf. Electron. (ET)*, Sep. 2018, pp. 1–4.

[16] I. Jekova, S. Tabakov, I. Iliev, V. Tsibulko, and K. Kostikova, "Real-time detection of pace pulses in a single lead ECG," in *Proc. Comput. Cardiology Conf. (CinC)*, Dec. 2018, pp. 1–4.

[17] J. Jurco, F. Plesinger, J. Halamek, P. Jurak, M. Matejkova, P. Leinveber, and J. Lipoldova, "Precise pacing artefact detection," in *Proc. Comput. Cardiol. Conf. (CinC)*, Sep. 2016, pp. 761–764.

[18] B.-U. Kohler, C. Hennig, and R. Orglmeister, "The principles of software QRS detection," *IEEE Eng. Med. Biol. Mag.*, vol. 21, no. 1, pp. 42–57, Jan./Feb. 2002.

[19] J. P. Martinez, R. Almeida, S. Olmos, A. P. Rocha, and P. Laguna, "A wavelet-based ECG delineator: Evaluation on standard databases," *IEEE Trans. Biomed. Eng.*, vol. 51, no. 4, pp. 570–581, Apr. 2004.

[20] I. Silva, "Robust detection of heart beats in multimodal data," *Physiol. Meas.*, vol. 36, no. 8, p. 1629, 2015.

[21] E. Frank, "An accurate, clinically practical system for spatial vectorcardiography," *Circulation*, vol. 13, no. 5, pp. 737–749, May 1956.

[22] G. E. Dower, H. B. Machado, and J. A. Osborne, "On deriving the electrocardiogram from vectorcardiographic leads," *Clin. Cardiol.*, vol. 3, no. 2, pp. 87–95, 1980.

PHILIP HOYLAND received the master's degree in electrical engineering from the Ecole Supérieure d'Electricité (Supélec), France, in 2014, and the M.Sc. degree (Hons.) in biomedical engineering from the University of Oxford, in 2014. He is currently pursuing the Ph.D. degree in signal processing with the Diagnosis and Interventional Adaptive Imaging (IADI) Unit, Inserm (U1254), Université de Lorraine. He is also a Clinical Specialist of cardiac electrophysiology for Biosense Webster. His research interests include electrophysiology, and imaging and signal processing.

NÉFISSA HAMMACHE was born in Paris in June 1990. She received the M.D. degree in cardiology from the Université de Lorraine, in 2018. She is currently pursuing the degree in interventional rhythmology, thanks to a chief residency, with the Cardiology Unit, CHRU Nancy, France.

ALBERTO BATTAGLIA was born in Turin in January 1986. He received the degree *(cum laude)* in medicine from the University of Turin, in 2011. In 2017, he received the Fellowship *(cum laude)* in cardiology from the University of Turin. In 2017, he moved to France for an Electrophysiology Fellowship from the Pôle Cardiologie, CHRU Nancy, Nancy, France, under the direction of Prof. Christian de Chillou. His research interests include the mechanisms of ventricular and supraventricular arrhythmias, and interventional electrophysiology.

JULIEN OSTER received the master's degree in electrical engineering, the master's degree in fundamental and applied mathematics from the Ecole Supérieure d'Electricité (Supélec), France, in 2006 and 2007, respectively, and the Ph.D. degree from the Université de Lorraine, Nancy, France, in 2009. In 2010, he was with the Centre Suisse d'Electronique and also with the Microtechnique (CSEM), Neuchâtel, Switzerland, where he was involved in the development of wearable technology. He received the Newton International Fellowship from the Royal Society, in 2010. He joined the University of Oxford, U.K. Since 2016, he has been a senior Research Fellow of Inserm (French Institute of Biomedical Research and Human Health), IADI Lab (U1254), Nancy, France. His research interests include the use of modeling and signal processing methods to extract novel clinical parameters and the use of machine learning techniques to provide predictive actionable information to clinicians.

JACQUES FELBLINGER (Member, IEEE) received the master's degree in biological and medical engineering in Nancy, France, the Ph.D. degree in instrumentation and signal processing in 1990, and the M.B.A. degree. His algorithm on the automatic detection of ventricular fibrillation, developed during his thesis, equips the automatic defibrillators of the Schiller Company (150 000 devices sold). From 1991 to 2001, he was with the University of Bern, where he developed several MRI-compatible devices and also developed cerebral and cardiac H1 spectroscopy. Following a second postdoctorate in neurosciences, he obtained a position as a Professor of medical imaging with the University of Nancy, in 2001. In 2005, he created the Diagnostic and Interventional Adaptive Imaging (IADI) Laboratory, which became a joint University-INSERM Unit. The laboratory specializes in the development of innovative instrumentation and methods for MRI. In 2008, it created the Clinical Investigation and Technological Innovation Centre (CIC-IT) for the validation and enhancement of medical devices in an MRI environment. In 2012, he founded the company Healtis, which offers solutions for validating the MRI compatibility of medical devices. Since his beginnings in MRI, he has been very involved in the safety aspects of MRI.

CHRISTIAN DE CHILLOU received the M.D. and Ph.D. degrees from Nancy University and the degree in cardiology in 1990. In the early 90's, he was a Fellow of electrophysiology with the Department of Cardiology, University Hospital of Maastricht, The Netherlands, headed by Prof. Hein Wellens. He is currently the Head of the Clinical Electrophysiology Unit, CHRU Nancy, France. He has authored more than 250 original articles, abstracts, and book chapters mainly focusing on clinical arrhythmia, electrophysiology, and radiofrequency catheter ablation. In 1998, he was honored with the Prix Medtronic for research on clinical arrhythmia. He is a member of the French Society of Cardiology, of the European Society of Cardiology, and of the European Heart Rhythm Association. He actively participates in the EHRA educational program for several years.

FREDDY ODILLE received the Ph.D. degree from Nancy University, Nancy, France, in 2007. In 2011, he was appointed as a Research Fellow of Inserm (French Institute of Healthcare Research), IADI Team, Nancy. Since 2015, he has also been with Nancy University Hospital, Nancy. He is currently the Deputy Head of IADI. His research interests include magnetic resonance imaging, image reconstruction, biomedical signal and image processing, and cardiac electrophysiology modeling and intervention.